Digital Communication Techniques

Signal Design and Detection

中　册

Marvin K. Simon
Jet Propulsion Laboratory

Sami M. Hinedi
Jet Propulsion Laboratory

William C. Lindsey
LinCom Corporation
University of Southern California

P T R Prentice Hall
Englewood Cliffs, New Jersey 07632

Digital Communication Techniques

Signal Design and Detection

中

Marvin K. Simon
Jet Propulsion Laboratory

Sami M. Hinedi
Jet Propulsion Laboratory

William C. Lindsey
LinCom Corporation
University of Southern California

PTR Prentice Hall
Englewood Cliffs, New Jersey 07632

Chapter 5

Noncoherent Communication with Waveforms

So far, we have concentrated on communication scenarios where a message is transmitted using a distinct signal that is precisely known to the receiver, except for the corrupting noise. In Chapter 4, it was shown that coherent demodulation involved mixing the received signal with inphase (I) and quadrature (Q) sinusoidal references, whose phases were exactly equal to the incoming received phase. It was shown that lack of knowledge of the incoming phase can result in cross-talk between the I and Q arms, the amount of which depends on the value of the carrier phase error ϕ, that is, the phase error between the locally generated and the incoming phase.

In many applications, it is not possible to perform coherent detection due to the inability of the receiver to produce meaningful carrier phase estimates, due, for example, to significant oscillator phase noise instability. In some scenarios, coherent systems are undesirable due to the additional complexity imposed by the phase estimation circuitry. In this chapter, we investigate noncoherent waveform communications in AWGN channels. First, we derive the structure and analyze the performance of optimum and suboptimum receivers in random phase channels. Both orthogonal and nonorthogonal signals are considered and the effects of imperfect time and/or frequency synchronization are assessed. We later extend the concept to both random amplitude and phase channels in which the amplitude of the incoming signal is also random due to fading in the link. Communications in both Rayleigh and Rician channels are examined and their respective performances evaluated.

In noncoherent M-ary communications, the received signal can be expressed by

$$\begin{aligned} m_0 \rightarrow H_0: &\quad r(t) = s_0(t, \boldsymbol{\Psi}) + n(t), \quad 0 \le t \le T \\ m_1 \rightarrow H_1: &\quad r(t) = s_1(t, \boldsymbol{\Psi}) + n(t), \quad 0 \le t \le T \\ &\vdots \\ m_{M-1} \rightarrow H_{M-1}: &\quad r(t) = s_{M-1}(t, \boldsymbol{\Psi}) + n(t), \quad 0 \le t \le T \end{aligned} \tag{5.1}$$

where the vector $\boldsymbol{\Psi}$ denotes the vector of unknown parameters [1] that are not or cannot be estimated in the receiver. As before, the noise is white Gaussian with one-sided PSD N_0 Watts/Hz and T denotes the duration of the transmitted message. We assume for now that perfect symbol synchronization has been achieved. Later, we will consider and assess the error probability in the presence of symbol sync error. Note that due to the randomness of the vector $\boldsymbol{\Psi}$, each message is transmitted using a sample waveform of a random process rather than a deterministic and known signal. As far as the receiver is concerned, it does not

distinguish between an unknown random phase introduced in the channel or a random phase inserted at the transmitter. A message m_i can be conveyed using a set or a family of known waveforms, rather than a fixed and unique waveform. Note that for a fixed vector $\boldsymbol{\Psi}$, the received waveforms are known precisely to the receiver. Hypothesis testing as described by (5.1) is typically referred to as "nonsimple" detection as opposed to the "simple" detection in coherent communications.

5.1 NONCOHERENT RECEIVERS IN RANDOM PHASE CHANNELS

In random phase channels, the phase θ of the received signal is not known, nor estimated by the receiver. All the other parameters such as amplitude and frequency are assumed known and hence, the vector $\boldsymbol{\Psi}$ of unknown parameters consists solely of the scalar θ, that is, $\boldsymbol{\Psi} = \theta$. The received signal, assuming m_i is transmitted, is thus given by[1]

$$r(t) = \sqrt{2}a_i(t)\cos(\omega_c t + \phi_i(t) + \theta) + n(t), \quad 0 \le t \le T \tag{5.2}$$

where ω_c is the carrier frequency, $a_i(t)$ the amplitude information, $\phi_i(t)$ the phase information[2], θ the unknown phase, and $n(t)$ the bandpass Gaussian noise process given by (4B.33) as

$$n(t) = \sqrt{2}\{n_c(t)\cos\omega_c t - n_s(t)\sin\omega_c t\} \tag{5.3}$$

The baseband noise components $n_c(t)$ and $n_s(t)$ are independent Gaussian processes with PSDs given by

$$S_{n_c}(f) = S_{n_s}(f) = \begin{cases} \frac{N_0}{2} & |f| \le B \\ 0 & \text{otherwise} \end{cases} \tag{5.4}$$

Now according to the bandpass sampling theorem [2], $n(t)$ is completely characterized by samples of $n_c(t)$ and $n_s(t)$ taken every $1/2B$ sec, that is

$$n(t) = \sqrt{2}\sum_{k=-\infty}^{\infty} \text{sinc}(2Bt - k)\{n_c(t_k)\cos\omega_c(t - t_k) - n_s(t_k)\sin\omega_c(t - t_k)\} \tag{5.5}$$

Moreover, we note that

$$\int_{-\infty}^{\infty} n^2(t)dt = \frac{1}{2B}\sum_{k=-\infty}^{\infty}\left\{n_c^2(t_k) + n_s^2(t_k)\right\} \tag{5.6}$$

represents the energy in the sample function $n(t)$. The joint pdf of the vector $\mathbf{n} = (n_c(t_1), n_c(t_2), \ldots, n_c(T), n_s(t_1), n_s(t_2), \ldots, n_s(T))^T$ created from sampling a T-second segment of $n(t)$ is given by

$$f_{n_c(t_1),\cdots,n_s(T)}(\mathbf{n}) = C\exp\left\{-\frac{\sum_{k=1}^{2BT}(n_c^2(t_k) + n_s^2(t_k))}{2N_0B}\right\} \tag{5.7}$$

1. As in Chapter 4, we denote the received random process by $r(t)$ and a sample function of that random process by $\rho(t)$. Similarly, the received random vector is denoted by $\mathbf{r}$ and a sample vector of that random vector by $\boldsymbol{\rho}$.

2. In Chapter 5, $\phi_i(t)$ denotes the phase information when message m_i is transmitted, but it also denotes the i^{th} basis function of the K-L expansion (consistent with the notation used in Chapter 4). The reader is therefore alerted to the dual use of $\phi_i(t)$ and special care is taken to redefine $\phi_i(t)$ whenever it is used.

since the $2 \times 2BT$ samples are uncorrelated, Gaussian each with variance N_0B. The constant C is the normalization factor such that the multidimentional integral of the density is unity. Using (5.6) to convert from sums of samples to a time integral, we have

$$f_{n_c(t_1),\ldots,n_s(T)}(\mathbf{n}) \simeq C \exp\left\{-\frac{1}{N_0}\int_0^T n^2(t)dt\right\} \tag{5.8}$$

which is identical to (4.7). Assuming that message m_i is transmitted and conditioning on the random phase θ, then

$$\begin{aligned} f_{\mathbf{r}}(\boldsymbol{\rho}/m_i,\theta) &= f_{\mathbf{n}}(\boldsymbol{\rho}-\mathbf{s_i}/m_i,\theta) = f_{\mathbf{n}}(\boldsymbol{\rho}-\mathbf{s_i}) \\ &= C\exp\left\{-\frac{\int_0^T\left(\rho(t)-\sqrt{2}a_i(t)\cos(\omega_c t+\phi_i(t)+\theta)\right)^2 dt}{N_0}\right\} \end{aligned} \tag{5.9}$$

and

$$f_{\mathbf{r}}(\boldsymbol{\rho}/m_i) = \int_{-\pi}^{\pi} f_{\mathbf{r}}(\boldsymbol{\rho}/m_i,\theta) f_{\theta/m_i}(\theta/m_i)d\theta \tag{5.10}$$

Assuming that θ is random and independent of which message is transmitted, $f_{\theta/m_i}(\theta/m_i) = f_\theta(\theta)$ and (5.10) simplifies to

$$f_{\mathbf{r}}(\boldsymbol{\rho}/m_i) = \int_{-\pi}^{\pi} f_{\mathbf{r}}(\boldsymbol{\rho}/m_i,\theta) f_\theta(\theta)d\theta \tag{5.11}$$

Since the receiver does not attempt to estimate the incoming phase θ, it can be assumed random with a uniform pdf, that is

$$f_\theta(\theta) = \begin{cases} \frac{1}{2\pi} & -\pi \le \theta \le \pi \\ 0 & \text{otherwise} \end{cases} \tag{5.12}$$

Expanding (5.9), $f_{\mathbf{r}}(\boldsymbol{\rho}/m_i,\theta)$ can be expressed as

$$f_{\mathbf{r}}(\boldsymbol{\rho}/m_i,\theta) = C'\exp\left\{\frac{2}{N_0}(z_{ci}\cos\theta - z_{si}\sin\theta)\right\}\exp\left(-\frac{E_i}{N_0}\right) \tag{5.13}$$

where $E_i = \int_0^T a_i^2(t)dt$ is the energy of $a_i(t)$ and the I-Q projections generated by means of a local oscillator are

$$z_{ci} = \int_0^T \rho(t)a_i(t)\sqrt{2}\cos(\omega_c t+\phi_i(t))dt \tag{5.14a}$$

$$z_{si} = \int_0^T \rho(t)a_i(t)\sqrt{2}\sin(\omega_c t+\phi_i(t))dt \tag{5.14b}$$

As a special case when the transmitted information is contained in the amplitude only, then $r(t) = \sqrt{2}s_i(t)\cos(\omega_c t+\theta)+n(t)$, that is, $\phi_i(t) = 0\ \forall i$ and $s_i(t) = a_i(t)$ and (5.14) can be expressed as the I-Q projections

$$z_{ci} = \int_0^T \rho_c(t)s_i(t)dt \tag{5.15a}$$

$$z_{si} = \int_0^T \rho_s(t)s_i(t)dt \tag{5.15b}$$

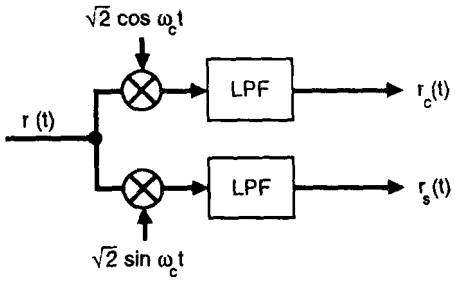

Figure 5.1 Demodulation with random phase

where

$$\rho_c(t) \triangleq \rho(t)\sqrt{2}\cos\omega_c t \tag{5.16a}$$

$$\rho_s(t) \triangleq \rho(t)\sqrt{2}\sin\omega_c t \tag{5.16b}$$

are the projections [inphase and quadrature (I and Q)] of the received waveform $\rho(t)$ onto the orthonormal basis $\{\sqrt{2}\cos\omega_c t, \sqrt{2}\sin\omega_c t\}$, as depicted in Fig. 5.1.

Transforming z_{ci} and z_{si} of (5.14) into polar coordinates using the envelope ξ_i and the phase ϕ_i as

$$z_{ci} = \xi_i \cos\phi_i \tag{5.17a}$$

$$z_{si} = \xi_i \sin\phi_i \tag{5.17b}$$

then

$$\begin{aligned} z_{ci}\cos\theta - z_{si}\sin\theta &= (\xi_i\cos\phi_i)\cos\theta - (\xi_i\sin\phi_i)\sin\theta \\ &= \xi_i\cos(\theta+\phi_i) \end{aligned} \tag{5.18}$$

and (5.13) becomes

$$f_{\mathbf{r}/\theta}(\boldsymbol{\rho}/m_i,\theta) \sim \exp\left\{\frac{2\xi_i}{N_0}\cos(\theta+\phi_i)\right\}\exp\left(-\frac{E_i}{N_0}\right) \tag{5.19}$$

Averaging over the density of θ, we have from (5.11) and (5.13)

$$f_{\mathbf{r}}(\boldsymbol{\rho}/m_i) \sim \frac{1}{2\pi}\int_{-\pi}^{\pi}\exp\left\{\frac{2\xi_i}{N_0}\cos(\theta+\phi_i)\right\}d\theta\exp\left(-\frac{E_i}{N_0}\right) \tag{5.20}$$

Such an integral has been encountered in several engineering applications and is referred to as the "zero-order modified Bessel function of the first kind" [3, 4]. Specifically, it is defined through

$$I_0(x) \triangleq \frac{1}{2\pi}\int_{-\pi}^{\pi} e^{x\cos\beta}d\beta \tag{5.21}$$

and is plotted in Fig. 5.2 as a function of x. For positive x, it is a monotonically increasing function and because of the periodicity of the cosine, an arbitrary phase ϕ can be added to its argument without altering the value of $I_0(x)$, that is

$$I_0(x) = \frac{1}{2\pi}\int_{-\pi}^{\pi} e^{x\cos(\beta+\phi)}d\beta \tag{5.22}$$

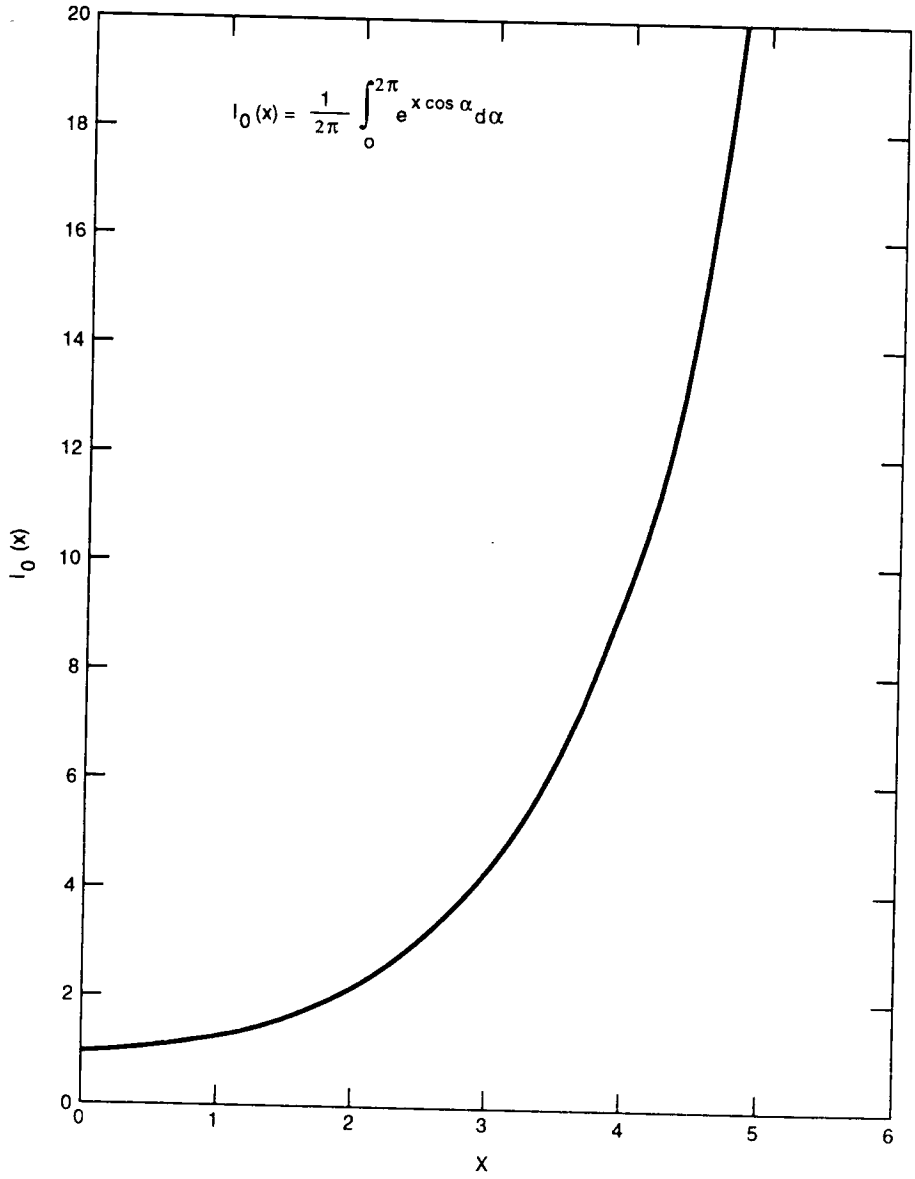

Figure 5.2 Plot of $I_0(x)$

Hence, using (5.22) in (5.20), the optimum decision rule sets $\hat{m}(\rho(t)) = m_k$ when

$$I_0\left(\frac{2\xi_i}{N_0}\right)\exp\left(-\frac{E_i}{N_0}\right) \tag{5.23}$$

is maximum for $k = i$. Recall from (5.17) that the envelope ξ_i is given by

$$\xi_i = \sqrt{z_{ci}^2 + z_{si}^2} \tag{5.24}$$

where z_{ci} and z_{si} are the projections of $\rho_c(t)$ and $\rho_s(t)$ onto the ith signal as given by (5.15a) and (5.15b), respectively. For equal energy signals, the factor $\exp(-E_i/N_0)$ can be ignored and since $I_0(2\xi_i/N_0)$ is a monotone increasing function, we need only to maximize ξ_i or ξ_i^2 where

$$\xi_i^2 = z_{ci}^2 + z_{si}^2 \tag{5.25}$$

The optimum receiver for equal energy signals is depicted in Fig. 5.3 where the received signal is first mixed with sine and cosine waveforms at the incoming frequency and the resulting outputs are correlated with each of the M possible transmitted signals.[3] The receiver then forms the sum of the squares of the sine and cosine correlations and decides on the message with maximum resulting envelope. It is clear that the decision process involves nonlinear operations unlike the coherent receiver discussed in Chapter 4. This is the penalty paid for not knowing or estimating the incoming carrier phase θ. An alternative implementation can be obtained with matched filters with impulse responses

$$h_i(t) = s_i(T - t), \quad i = 0, 1, \cdots, M - 1 \tag{5.26}$$

followed by a sampler at multiples of T seconds as shown in Fig. 5.4. When the signals can be expressed as

$$s_i(t) = \sum_{j=1}^{N} s_{ij}\phi_j(t), \quad i = 0, 1, \cdots, M - 1 \tag{5.27}$$

as given by (4.40), then it is possible to correlate $r_c(t)$ and $r_s(t)$ with the basis functions $\phi_i(t), i = 1, 2, \cdots, N$ and apply the appropriate signal weights to form the various ξ_i^2, $i = 0, 1, \cdots, M - 1$, as shown in Fig. 5.5.

A significantly different approach for optimum detection of equiprobable equal energy signals is possible with envelope detectors. Consider Fig. 5.6, which depicts a filter $h_{bp,k}(t)$ followed by an envelope detector. Since the input to the filter $r(t)$ is centered at f_c, let the filter $h_{bp,k}(t)$ be matched to the signal $s_k(t)$, translated to frequency f_c ("bp" stands for bandpass), that is

$$h_{bp,k}(t) \triangleq \sqrt{2}s_k(T - t)\cos\omega_c t, \quad k = 0, 1, \cdots, M - 1 \tag{5.28}$$

The output of the filter becomes

$$\begin{aligned} u_k(t) &= \int_{-\infty}^{\infty} r(\tau)h_{bp,k}(t - \tau)d\tau \\ &= \sqrt{2}\int_{-\infty}^{\infty} r(\tau)s_k(T - t + \tau)\cos\omega_c(t - \tau)d\tau \end{aligned} \tag{5.29}$$

or

$$u_k(t) = u_{ck}(t)\cos\omega_c t + u_{sk}(t)\sin\omega_c t \tag{5.30}$$

3. Note that in Fig. 5.3, lowpass filters have been inserted at the output of the mixers. As long as the bandwidth of these filters is much larger than the data rate, they do not impact the performance of the optimum receiver. It is however good practice to include them in an analog implementation as the mixers are highly nonlinear devices that generate more than the desired product at their output.

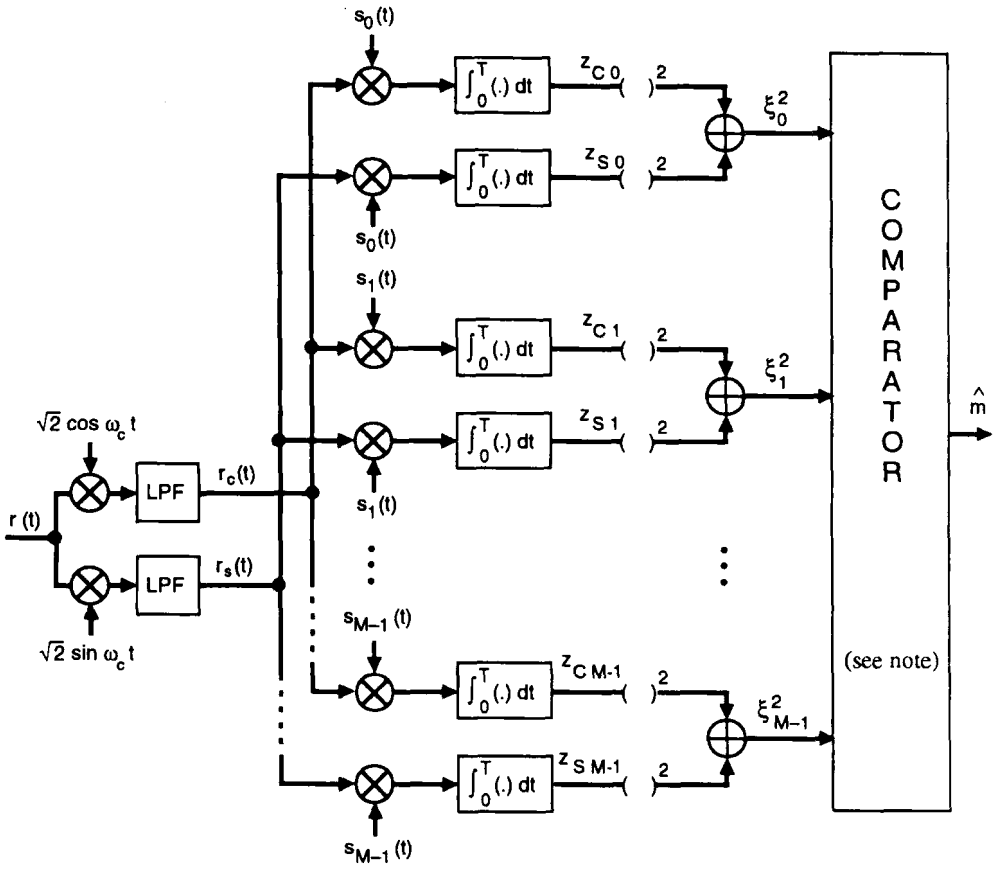

Note: From here on, a "**comparator**" selects the message corresponding to maximum input value or voltage.

Figure 5.3 M-ary noncoherent receiver for equal energy signals

where we define

$$u_{ck}(t) \triangleq \int_{-\infty}^{\infty} r(\tau)s_k(T-t+\tau)\sqrt{2}\cos\omega_c\tau\,d\tau = \int_{-\infty}^{\infty} r_c(\tau)s_k(T-t+\tau)d\tau \quad (5.31a)$$

$$u_{sk}(t) \triangleq \int_{-\infty}^{\infty} r(\tau)s_k(T-t+\tau)\sqrt{2}\sin\omega_c\tau\,d\tau = \int_{-\infty}^{\infty} r_s(\tau)s_k(T-t+\tau)d\tau \quad (5.31b)$$

Since $r_c(\tau)$ and $r_s(\tau)$ are low-frequency signals and $s_k(\tau)$ is also a slowly varying signal, both $u_{ck}(t)$ and $u_{sk}(t)$ remain relatively constant over several cycles of $\cos\omega_c t$. As a result, $u_k(t)$ is a bandpass signal and can thus be expressed as

$$u_k(t) = \mathrm{Re}\left\{a_k(t)e^{-j\omega_c t}\right\} \quad (5.32)$$

where the complex baseband waveform $a_k(t)$ is given by

$$a_k(t) = u_{ck}(t) + ju_{sk}(t) \quad (5.33)$$

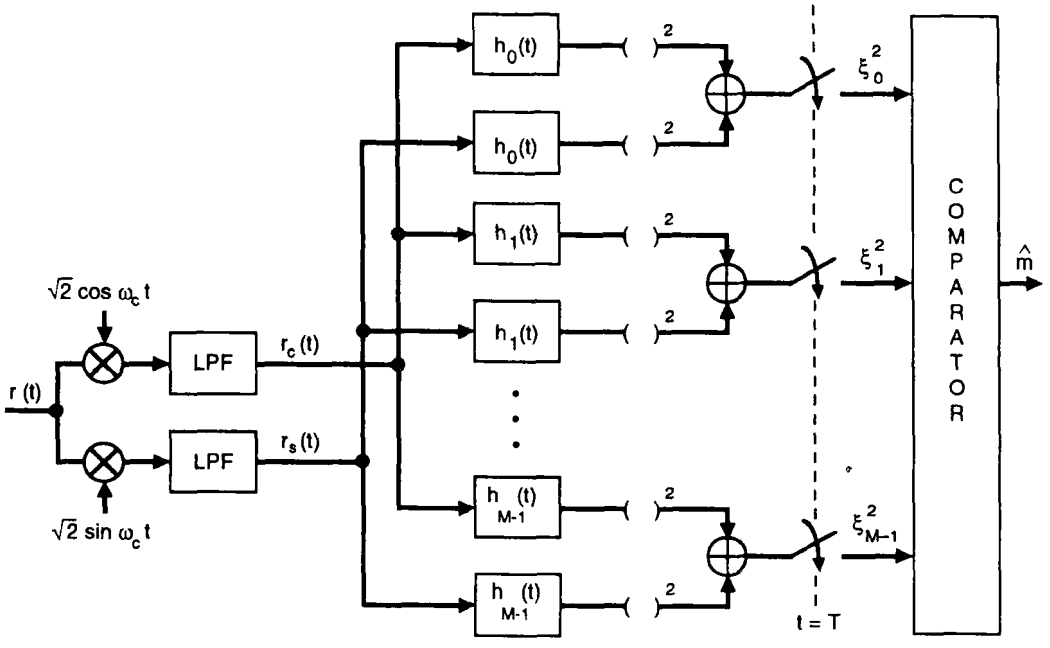

Figure 5.4 Alternate implementation of M-ary noncoherent receivers for equal energy signals with matched filters

The output of the envelope detector becomes

$$e_k(t) = |a_k(t)| \tag{5.34a}$$

or

$$e_k(t) = \sqrt{u_{ck}^2(t) + u_{sk}^2(t)} \tag{5.34b}$$

If we sample the output at $t = T$, we have from (5.34) and (5.31)

$$\begin{aligned} e_k(T) &= \sqrt{u_{ck}^2(T) + u_{sk}^2(T)} \\ &= \sqrt{\left(\int_0^T r_c(\tau)s_k(\tau)d\tau\right)^2 + \left(\int_0^T r_s(\tau)s_k(\tau)d\tau\right)^2} \end{aligned} \tag{5.35}$$

which is identical to ξ_k as given by (5.24) since $u_{ck}(T) = z_{ck}$ and $u_{sk}(T) = z_{sk}$ as given by (5.15a) and (5.15b), respectively. Hence, the optimum M-ary noncoherent detector for equiprobable, equal energy signals can be implemented using matched filters (to the bandpass rather than the baseband signals) and envelope detectors as shown in Fig. 5.7. Receivers that examine only the envelope of the matched filter output are termed *noncoherent* or *incoherent receivers* as they do not exploit the knowledge of the carrier phase; receivers that do exploit knowledge of the carrier phase are called *coherent*.

5.1.1 Optimum *M*-FSK Receivers

A signal set of great interest in noncoherent communications consists of M sinusoids at distinct frequencies and the set is referred to as *Multiple Frequency-Shift-Keying* (M-FSK) signals. In general, the frequency separation can be nonuniform, but equidistant signals are

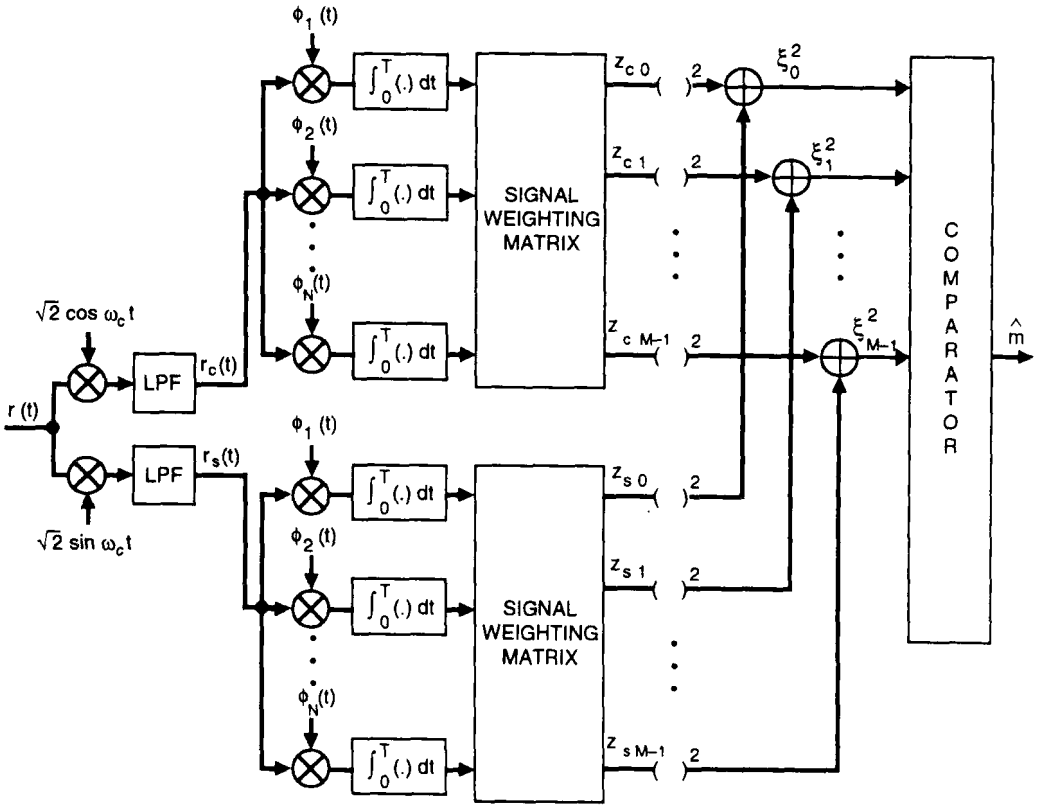

Figure 5.5 M-ary noncoherent receiver implementation with the basis functions

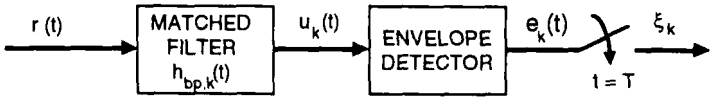

Figure 5.6 Envelope detection

of great practical interest as they occupy the minimum required bandwidth for orthogonal noncoherent communications. The transmitted signals are characterized by

$$s_k(t) = \sqrt{2P}\cos(\omega_c t + \omega_k t + \theta), \quad 0 \le t \le T \tag{5.36}$$

where ω_k denotes the frequency of the kth tone and θ the unknown random phase. The latter is independent from message to message because each signal is typically generated by a unique oscillator whose initial phase is random when the signal is selected. The pairwise signal correlation coefficient, as defined by (4.45), reduces to

$$\gamma_{ij} = \frac{1}{E}\int_0^T s_i(t)s_j(t)dt = \frac{1}{T}\int_0^T \cos(2\pi f_{i,j}t + \theta - \theta')dt \tag{5.37}$$

where $E = PT$, $f_{i,j} = f_i - f_j$ is the frequency separation between the tones, and θ, θ'

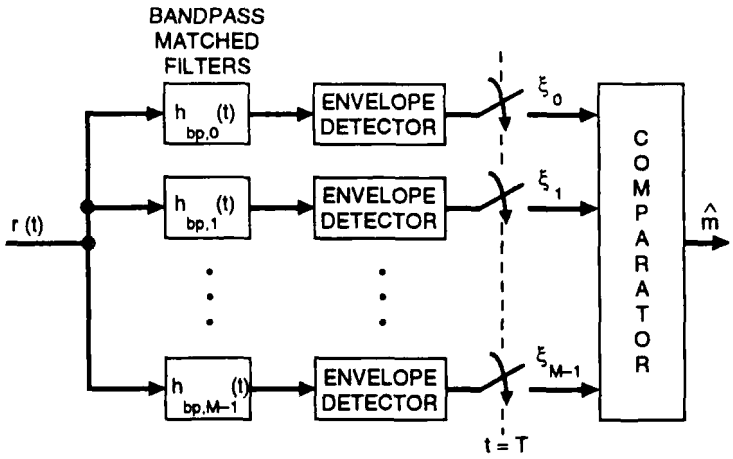

Figure 5.7 Envelope detector noncoherent receiver for equal energy signals

are the random carrier phases when signals $s_i(t)$ and $s_j(t)$ are transmitted. Because of the random phase $\theta - \theta'$, the only way to guarantee zero correlation is for the integral to be carried out over at least a full period of the difference sinusoid. Hence, the minimum frequency separation to guarantee orthogonality is

$$f_{i,j} = \frac{1}{T} \text{ Hz} \tag{5.38}$$

This separation is equal to twice the minimum separation required for coherent M-FSK transmission, $1/(2T)$, derived earlier in Chapter 4. Given M tones, the minimum bandwidth required for orthogonal noncoherent transmission is M/T Hz achieved by uniformly spacing the tones with $1/T$ Hz separation. The received signal, assuming that message m_k is transmitted, is given by

$$r(t) = \sqrt{2P}\cos\left(2\pi f_c + 2\pi\left(\frac{k}{T}\right)t + \theta\right) + n(t), \quad 0 \le t \le T \tag{5.39}$$

Typically, the tones are symmetrically spaced around the carrier f_c, which can easily be modeled by (5.39) by considering negative values of k. The optimum receiver is still as shown in Fig. 5.3 where the various signals are the corresponding sinusoids. The receiver still computes ξ_i^2 for each signal using $\xi_i^2 = z_{ci}^2 + z_{si}^2$ where z_{ci} and z_{si} are given by (5.14) with $a_i(t) = \sqrt{P}\ \forall i$ and $\phi_i(t) = \omega_i t\ \forall i$, that is

$$z_{ci} = \sqrt{2P}\int_0^T r(t)\cos(\omega_c + \omega_i)t\,dt \tag{5.40}$$

and

$$z_{si} = \sqrt{2P}\int_0^T r(t)\sin(\omega_c + \omega_i)t\,dt \tag{5.41}$$

Hence

$$\xi_i^2 = 2P\left\{\left(\int_0^T r(t)\cos(\omega_c + \omega_i)t\,dt\right)^2 + \left(\int_0^T r(t)\sin(\omega_c + \omega_i)t\,dt\right)^2\right\} \tag{5.42}$$

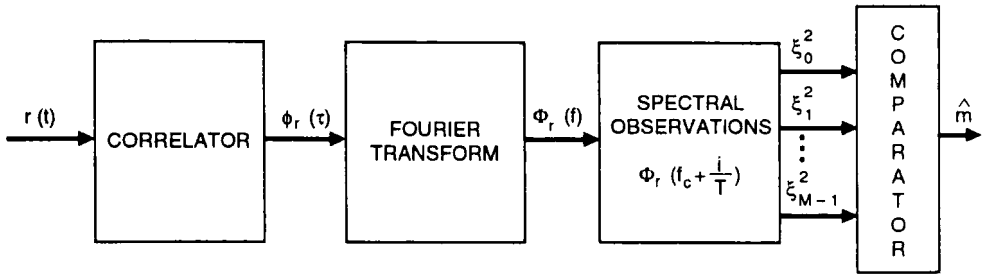

Figure 5.8 Highpass spectrum analyzer receiver

Using the procedure outlined in Appendix 5B, (5.42) is identically equivalent to

$$\xi_i^2 = 4P \int_0^T \int_0^{T-\tau} r(t)r(t+\tau)\cos(\omega_c + \omega_i)\tau d\tau dt \tag{5.43}$$

Defining the finite-time autocorrelation function of $r(t)$ as

$$\phi_r(\tau) \triangleq \int_0^{T-\tau} r(t)r(t+\tau)dt, \quad 0 \le \tau \le T \tag{5.44}$$

then, (5.43) can be expressed as

$$\xi_i^2 = 4P \int_0^T \phi_r(\tau)\cos(\omega_c + \omega_i)\tau d\tau \tag{5.45}$$

Following the argument in Appendix 5B, the quantity ξ_i^2 can be viewed as the Fourier transform of the even function $\phi_{e,r}(\tau)$ [constructed from $\phi_r(\tau)$ as in (5B.10)] evaluated at the discrete frequency $f_c + f_i$; thus

$$\xi_i^2 = 4P\Phi_{e,r}(f_c + f_i) \tag{5.46}$$

where $\Phi_{e,r}(f)$ denotes the Fourier transform [5] of $\phi_{e,r}(\tau)$. This interpretation of the decision process leads to the the highpass spectrum analyzer receiver in Fig. 5.8.[4] In practice, the received signal is first downconverted to an equivalent lowpass waveform $v(t)$ using a reference at the carrier frequency. Thus, any practical implementation must be provided with an estimate of f_c. This heterodyning operation reduces the highpass spectrum analyzer receiver of Fig. 5.8 to its lowpass equivalent illustrated in Fig. 5.9, with the corresponding observations $\{\Phi_v(i/T),\ i = 0, 1, \cdots, M-1\}$.

5.1.2 Suboptimum *M*-FSK Receivers

Exact evaluation of the spectral observations is difficult when one elects to implement the spectrum analyzer receivers of Figures 5.8 and 5.9. However, it is possible to approximate the spectral estimate $\Phi_v(f)$ which then results in a receiver performance that is suboptimum. There are various approaches to approximating the spectral observations $\{\Phi_v(k/T),\ k = 0, 1, \cdots, M-1\}$.

First, one can evaluate the autocorrelation function $\phi_v(\tau)$ directly and then evaluate the Fourier transform to obtain $\Phi_v(f)$. This is referred to as the *autocorrelation function*

4. In Figures 5.8 and 5.9, the Fourier transform is operating on the resulting even function, as discussed in Appendix 5B.

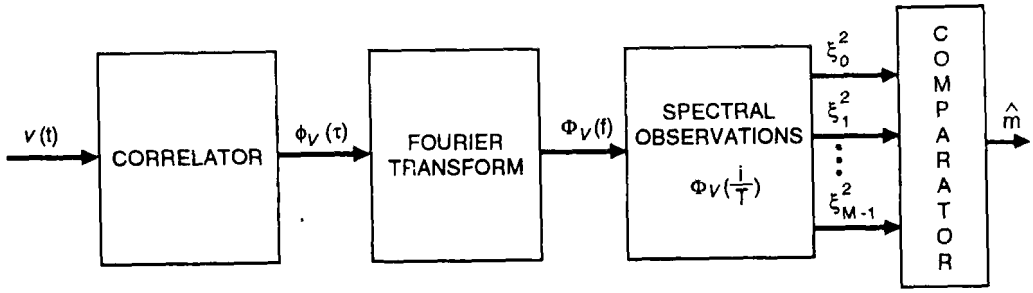

Figure 5.9 Lowpass spectrum analyzer receiver

method. A practical realization of this method that is convenient for digital processing is discussed in [6, 7] and summarized here. Since the Fourier transform of the random process $v(t)$ is essentially zero outside the frequency interval $|f| \leq M/T$, then in accordance with the sampling theorem we have, to a good approximation

$$v(t) \simeq v_a(t) \triangleq \sum_{n=1}^{2BT} v\left(\frac{n}{2B}\right) \operatorname{sinc}\left[2B\left(t - \frac{n}{2B}\right)\right] \tag{5.47}$$

where $B \triangleq M/T$ and $v_n = v(n/2B)$ is a sample of $v(t)$ at $t = n/2B$. In terms of the above, the autocorrelation function of $v_a(t)$ is given by

$$\phi_{v_a}(\tau) = \int_0^{T-\tau} v_a(t)v_a(t+\tau)dt = \sum_{n=1}^{2BT}\sum_{m=1}^{2BT} v_n v_m \operatorname{sinc}\left[2B\left(\tau + \frac{n-m}{2B}\right)\right] \tag{5.48}$$

which approximates that of $\phi_v(\tau)$. We observe that for $\tau = k/2B$, k an integer, the above expression simplifies to

$$\phi_{v_a}\left(\frac{k}{2B}\right) = \begin{cases} \frac{1}{2B}\sum_{n=1}^{2BT-k} v_n v_{n+k}, & k = 0, \pm 1, \pm 2, \cdots, \pm(2BT-1) \\ 0, & \text{otherwise} \end{cases} \tag{5.49}$$

Since the spectrum of $\phi_{v_a}(\tau)$ is limited to the frequency range $|f| \leq B$, one obtains by means of the sampling theorem

$$\phi_{v_a}(\tau) = \sum_{k=-(2BT-1)}^{2BT-1} \phi_{v_a}\left(\frac{k}{2B}\right) \operatorname{sinc}\left[2B\left(\tau - \frac{k}{2B}\right)\right] \tag{5.50}$$

Taking Fourier transforms, the spectrum of $v(t)$ is approximated by

$$\Phi_v(f) \simeq \Phi_{v_a}(f) = \frac{1}{2B}\phi_{v_a}(0) + \frac{1}{B}\sum_{k=1}^{2BT-1} \phi_{v_a}\left(\frac{k}{2B}\right)\cos\left(\frac{\pi k f}{B}\right), \quad -B \leq f \leq B \tag{5.51}$$

These expressions for the correlation coefficients and for the approximate spectral observations $\Phi_{v_a}(k/T)$ form the basis for the computational procedure.

Second, one can calculate the spectrum by the discrete Fourier transform approach. The latter takes samples $v(k/2B)$, $k = \{1, 2, \cdots, 2BT\}$ and evaluates

$$X(f) = \sum_{k=1}^{2BT} v\left(\frac{k}{2B}\right)\cos\left(\frac{\pi k f}{B}\right) \quad \text{and} \quad Y(f) = \sum_{k=1}^{2BT} v\left(\frac{k}{2B}\right)\sin\left(\frac{\pi k f}{B}\right) \tag{5.52}$$

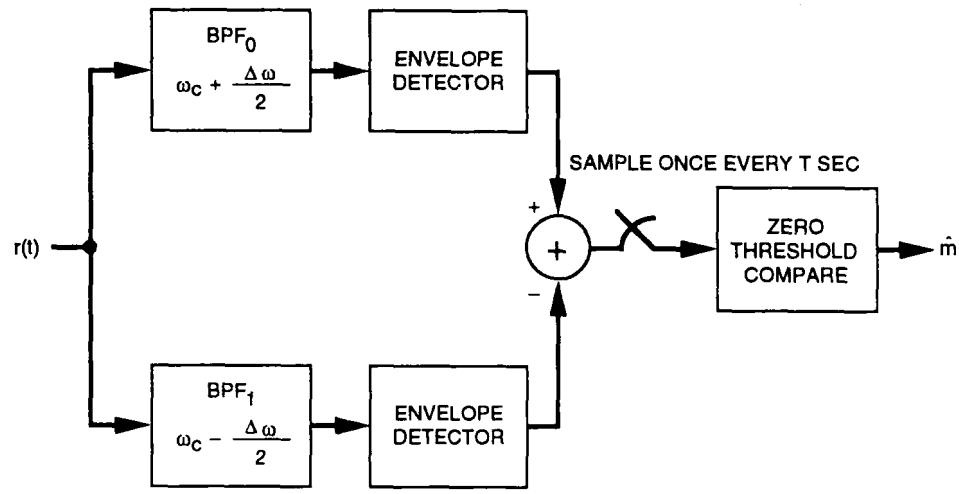

Figure 5.10 Suboptimum binary FSK receiver

and then computes the spectrum

$$\Phi_v(f) \simeq X^2(f) + Y^2(f) \tag{5.53}$$

which yields the spectral observations $\Phi_v(k/T)$, $k = \{1, 2, \cdots, 2BT\}$. The discrete Fourier transform method permits greatly simplified analysis [8].

Third, the receiver can be implemented with a small computer programmed with the *Cooley-Tukey* Fast Fourier Transform algorithm [9] and processing the output of an analog-to-digital converter. The Fast Fourier Transform (FFT) approach produces results at frequencies that are multiples of $1/T$ provided that the number of samples is a power of two. Although the FFT method does not give better results than the discrete Fourier transform or the autocorrelation function method, it has the advantage that considerably less time is required to perform numerical operations.

Suboptimum detection also occurs when there is a bandpass limiter prior to the detector. In many applications, bandpass limiters are used to provide some form of automatic gain control (AGC) in the receiver and because of their inherent nonlinearity, they degrade the performance of the detector. Suboptimum detection of binary FSK signals in the presence of a bandpass limiter is discussed in [10], where it is shown that a 0.5 dB degradation occurs for $P_s(E) \leq 10^{-2}$. Another form of suboptimum detection occurs when the integrate-and-dump filters are replaced by bandpass filters as shown in Fig. 5.10 for binary FSK signals, symmetrically located around the carrier frequency. In this case, the receiver performance is degraded and is a function of the bandpass filter bandwidth, as discussed later.

5.2 PERFORMANCE OF NONCOHERENT RECEIVERS IN RANDOM PHASE CHANNELS

It is of great interest to assess the performance of noncoherent systems and compare it to their coherent counterpart. First, we will derive the performance of orthogonal signals and determine the resulting penalty paid in not tracking the carrier phase at the receiver. We will then generalize the results to any arbitrary set of signals and in particular, consider

the effect of frequency and timing synchronization errors. A bound on the performance of orthogonal M-FSK signals is then presented in the presence of frequency error. Finally, the performances of two suboptimum M-FSK receivers are evaluated and the effect of time domain truncation in evaluating the spectral observations is assessed.

5.2.1 Performance of M-ary Orthogonal Signals

The M-ary receiver for equal energy signals is depicted in Fig. 5.3 and the receiver picks the message m_k corresponding to maximum ξ_i^2 for $i = 0, 1, \cdots, M-1$. In order to compute the probability of symbol error, we need to characterize the joint pdf $f_{\xi_0^2,\xi_1^2,\cdots,\xi_{M-1}^2}(\xi_0^2, \xi_1^2, \cdots, \xi_{M-1}^2)$. Assuming that message m_k is transmitted, then $r(t) = \sqrt{2}s_k(t)\cos(\omega_c t + \theta) + n(t)$ with

$$z_{ci} = \int_0^T r_c(t)s_i(t)dt = \int_0^T (s_k(t)\cos\theta + n_c(t))s_i(t)dt \tag{5.54}$$

and

$$z_{si} = \int_0^T r_s(t)s_i(t)dt = \int_0^T (s_k(t)\sin\theta + n_s(t))s_i(t)dt \tag{5.55}$$

For a fixed θ, the conditional means become

$$E\{z_{ci}/\theta\} = \cos\theta \int_0^T s_k(t)s_i(t)dt = \begin{cases} E_s\cos\theta, & i = k \\ 0, & i \neq k \end{cases} \tag{5.56}$$

Similarly

$$E\{z_{si}/\theta\} = \sin\theta \int_0^T s_k(t)s_i(t)dt = \begin{cases} E_s\sin\theta, & i = k \\ 0, & i \neq k \end{cases} \tag{5.57}$$

The conditional variances are computed using

$$\sigma^2_{z_{ci}/\theta} = E\left\{\left(\int_0^T n_c(t)s_i(t)dt\right)^2\right\} = \frac{N_0}{2}E_s \tag{5.58a}$$

and

$$\sigma^2_{z_{si}/\theta} = E\left\{\left(\int_0^T n_s(t)s_i(t)dt\right)^2\right\} = \frac{N_0}{2}E_s \tag{5.58b}$$

which are also the unconditional variances. Recall that $n_c(t)$ and $n_s(t)$ are bandlimited processes; however, assuming that $BT \gg 1$, they can be viewed as nonbandlimited using the matched filter argument previously outlined in Chapter 4. Since $n_c(t)$ and $n_s(t)$ are independent, z_{ci} and z_{si} are conditionally uncorrelated and hence independent since they are conditionally Gaussian, that is

$$\begin{aligned} f_{z_{ci},z_{si}}(z, y/\theta) &= \frac{1}{\pi E_s N_0}\exp\left\{-\frac{(z - E\{z_{ci}/\theta\})^2 + (y - E\{z_{si}/\theta\})^2}{E_s N_0}\right\} \\ &= \begin{cases} \frac{1}{\pi E_s N_0}\exp\left\{-\frac{z^2+y^2}{E_s N_0}\right\}, & i \neq k \\ \frac{1}{\pi E_s N_0}\exp\left\{-\frac{z^2+y^2+E_s^2-2E_s z\cos\theta-2yE_s\sin\theta}{E_s N_0}\right\}, & i = k \end{cases} \end{aligned} \tag{5.59}$$

Consider now the pairwise correlation among the various z_{ci} and z_{si}, $i = 0, 1, \cdots, M-1$. Assuming that m_k is transmitted, then

$$\begin{aligned} E\{z_{ci}z_{cj}\} &= E\left\{\left[\int_0^T (s_k(t)\cos\theta + n_c(t))s_i(t)dt\right]\left[\int_0^T (s_k(\tau)\sin\theta + n_c(\tau))s_j(\tau)d\tau\right]\right\} \\ &= E\left\{\left(\int_0^T n_c(t)s_i(t)dt\right)\left(\int_0^T n_c(\tau)s_j(\tau)d\tau\right)\right\} \\ &= 0, \quad i \neq j, i \neq k, j \neq k \end{aligned} \tag{5.60}$$

Moreover

$$\begin{aligned} E\{z_{ck}z_{cj}\} &= E\left\{\left(E_s\cos\theta + \int_0^T n_c(t)s_k(t)dt\right)\left(\int_0^T n_c(\tau)s_j(\tau)d\tau\right)\right\} \\ &= 0, \quad j \neq k \end{aligned} \tag{5.61}$$

Using similar arguments, it can be easily shown that

$$\begin{aligned} E\{z_{si}z_{sj}\} &= E\{z_{si}\}E\{z_{sj}\} = 0, \quad i \neq j \\ E\{z_{ci}z_{sj}\} &= E\{z_{ci}\}E\{z_{sj}\} = 0, \quad i = j \end{aligned} \tag{5.62}$$

which holds true even when $i = k$ or $j = k$ but not both. Therefore, the variables z_{ci} and z_{si}, $i = 0, 1, \cdots, M-1$ are uncorrelated and hence independent since they are conditionally Gaussian. Defining $\theta_i = \tan^{-1}(z_{si}/z_{ci})$, then (5.59) becomes

$$f_{z_{ci},z_{si}}(z, y/\theta) = \begin{cases} \frac{1}{\pi E_s N_0}\exp\left\{-\frac{z^2+y^2}{E_sN_0}\right\}, & i \neq k \\ \frac{1}{\pi E_s N_0}\exp\left\{-\frac{z^2+y^2+E_s^2-2E_s\sqrt{z^2+y^2}\cos(\theta-\theta_i)}{E_sN_0}\right\}, & i = k \end{cases} \tag{5.63}$$

Integrating over θ and using the definition of $I_0(x)$ as given by (5.22), (5.63) reduces to

$$f_{z_{ci},z_{si}}(z, y) = \begin{cases} \frac{1}{\pi E_s N_0}\exp\left\{-\frac{z^2+y^2}{E_sN_0}\right\}, & i \neq k \\ \frac{1}{\pi E_s N_0}\exp\left\{-\frac{z^2+y^2+E_s^2}{E_sN_0}\right\} I_0\left(\frac{2\sqrt{z^2+y^2}}{N_0}\right), & i = k \end{cases} \tag{5.64}$$

Making the change of variables $\xi_i = \sqrt{z_{ci}^2 + z_{si}^2}$, then

$$f_{\xi_i}(\xi) = \begin{cases} \frac{2\xi}{E_sN_0}\exp\left\{-\frac{\xi^2}{E_sN_0}\right\}, & i \neq k \\ \frac{2\xi}{E_sN_0}\exp\left\{-\frac{\xi^2+E_s^2}{E_sN_0}\right\} I_0\left(\frac{2\xi}{N_0}\right), & i = k \end{cases} \tag{5.65}$$

The Rayleigh and Rician densities of (5.65) can also be obtained using the results of Appendix 5A, namely, (5A.21) and (5A.27) with $\sigma^2 = N_0E_s/2$ and $s^2 = E_s^2$. Let us proceed by normalizing ξ_i^2 using

$$A_i = \frac{\xi_i^2}{E_sN_0} \tag{5.66}$$

then $f_{A_i}(a)$ is given by

$$f_{A_i}(a) = \frac{f_{\xi_i}(\sqrt{E_sN_0a})}{2\sqrt{(a/E_sN_0)}} \tag{5.67}$$